TENTH AUSTRALASIAN FLUID MECHANICS
CONFERENCE - UNIVERSITY OF MELBOURNE
11-15 DECEMBER 1989

Keynote Paper KS-9

DISSOCIATING FLOWS IN HYPERVELOCITY AERODYNAMICS

R.J. STALKER

Department of Mechanical Engineering
University of Queensland
St. Lucia, QLD 4067
AUSTRALIA

ABSTRACT

Order of magnitude arguments are used to identify and explain some of the special effects associated with chemical dissociation in inviscid hypervelocity aerodynamics. This leads to three simplified, approximate, concepts, in the form of a constant temperature approximation, thermodynamic decoupling of the temperature from the flow, and pressure gradient reaction quenching. These concepts are illustrated by application to a range of classical problems in hypervelocity aerodynamics, namely, prediction of shock stand-off on a blunt body, the development of shock detachment on a wedge, the variation of shock stand-off on a delta wing, and the density variation along a streamline downstream of a curved shock.

1. INTRODUCTION

The real gas effects due to molecular vibration and dissociation, as well as ionization, are a feature of the flow fields associated with hypervelocity flight. In early years, the blunt body vehicle configurations which were used for flight in this regime followed trajectories such that the dominant real gas effects occurred with the gas in an equilibrium condition, and it is not surprising that the techniques developed for calculating these flows tended to use equilibrium thermodynamics models.

Another reason for using equilibrium real gas thermodynamics is that it can be viewed as a natural extension of the well known thermodynamics of perfect gas flows. In a set of equations which would describe a gas dynamic flow, the thermodynamic ones may be seen to have the role of providing a relationship between pressure and density which makes the equations of momentum and continuity yield a determinate solution. For both perfect gas and equilibrium real gas flows, the relationship involves only the local thermodynamic state variables at any point in the flow, and although it is far more complicated for an equilibrium real gas than for a perfect gas, the local dependence means that similar approaches can be used to study both types of flow. For example the method of characteristics, which has proven very useful in solving perfect gas problems, can be applied directly to the solution of equilibrium real gas flows, but is more difficult to apply to non-equilibrium flows.

Therefore, it may seem unfortunate that equilibrium does not prevail in all real gas flow fields, but such indeed is the case - as, for example, in the flow fields produced by the new generation of hypervelocity vehicles, such as the Space Shuttle or Aero-assisted Orbital Transfer Vehicles. This can be seen by reference to Fig. 1, where the region on a velocity altitude diagram is shown in which non-equilibrium is expected, downstream of a 40^0 shock or a normal shock for a distance which is comparable with the dimensions of a normal flight vehicle. The 40^0 shock and the normal shock have been chosen as representative of the shock preceding a major part of the flow field for a re-entry glider and an A.O.T.V. respectively. Above the upper boundary for the 40^0 shock, reactions are so slow that no significant effect takes place for a distance of 1 m or greater after a sample of air crosses the shock, so the flow is effectively "frozen", and behaves as a perfect gas. Below the lower boundary, reactions are so fast that equilibrium is achieved within 1 m after crossing the shock, and the flow behaves as an equilibrium real gas. It can be seen that the trajectory for a re-entry glider is such that it is well removed from either boundary, and flies in a truly non-equilibrium regime. Similar arguments apply to the A.O.T.V., which experiences its major force and heat transfer loads in the non-equilibrium regime.

Thus, it appears that yet another complication has been introduced into these flow fields, in that not only are the local state variables related in a relatively complex manner, but they also depend upon the time history of the flow along the streamlines. In fact, the nature of the time dependence offers the prospect of making some simplifications to the models describing the flow which, although they are approximate do allow the main features of some important flow situations to be determined. This simplified and approximate approach is discussed in this paper.

Noting that equilibrium is achieved by backward (i.e. recombination) reaction rates rising to values such that they match the forward rates, it follows that the wide separation between the flight trajectory and the equilibrium boundary on Fig. 1 indicates the dominance of forward reactions in the vehicle flow field. Thus, the discussion considers only flows in which the backward reaction are neglected.

Further, only the flow downstream of a strong shock is discussed, since the flow field about the configurations of interest generally will be preceded by a strong shock. This is not a serious limitation, since a strong shock will usually be needed in order to give rise to real gas effects, and it may even include cases such as could occur on a slender acceleration vehicle at low angle of incidence, where non-reacting flow over the main part of the vehicle may be followed by local areas of reacting flow, as at the leading edge of a fin.

Finally vibration and ionization effects are neglected. For speeds up to Earth orbital

velocities, this is a good approximation, since the energy involved in dissociation usually considerably outweighs the other two. In addition, the dissociation process is represented by the Lighthill-Freeman model (Freeman, 1958) of an ideal dissociating gas. This provides a good quantitative representation of the non-equilibrium behaviour of oxygen or nitrogen alone and, although the formation of nitric oxide renders it less accurate as a model for air, it does provide a good qualitative representation in that case as well.

2. ANALYSIS

For an ideal dissociating gas, the equation for the rate at which the gas dissociates in passing along a streamline after crossing a shock is written as

$$d\alpha/ds = C\, q^{-1}\, T^{-n}\, \rho(1-\alpha)\, \exp(-T^{-1}) \qquad (1)$$

where, as noted above, the recombination term has been neglected.

Putting

$$\xi = \int_0^s \rho q^{-1}\, ds \quad , \qquad (2)$$

this becomes

$$d\alpha/d\xi = CT^{-n}\,(1-\alpha)\,\exp(-T^{-1}) \quad . \qquad (3)$$

The variable ξ is referred to here as the binary reaction variable. It can be seen as a measure of the cumulative number of collisions experienced by an average molecule as it passes along a streamline. As the number increases, the probability that the molecule is dissociated also increases, subject to the factors on the right hand side of Eqn. (1) which modify the efficiency with which collisions produce dissociation.

The exponential term is dominant amongst the factors which influence collision efficiency. It arises from the fact that only those molecules at the high energy end of the molecular Maxwellian velocity distribution have enough energy to experience dissociation when they collide with other molecules. Not only does this ensure that only a small fraction of the collisions occurring in the gas are dissociating ones but, because it also means that the energy of most of the molecules is insufficient for a dissociating collision, it follows that $T \ll 1$, and that the exponential term is very sensitive to temperature variation. This causes this factor to have a dominant effect on the rate of dissociation.

The enthalpy per unit mass of an ideal dissociating gas and the equation of state are written, respectively, as

$$h = D\{(4 + \alpha)T + \alpha) \qquad (4)$$

and

$$p = D\rho T(1 + \alpha) \quad . \qquad (5)$$

Thus, since the stagnation enthalpy, $h + 0.5\, q^2$, is constant along streamlines, and the momentum equation is

$$dp/d\xi = -\rho q\, dq/d\xi \quad ,$$

it follows that, along streamlines

$$(4 + \alpha)dT/d\xi = -(1 + T)d\alpha/d\xi + (\rho D)^{-1}\, dp/d\xi. \qquad (6)$$

Now, at normal flight densities, T is of the order of 0.05, which implies that the exponential term in Eqn. (3) is very sensitive to small variations in T. For example, a 5% change in T changes that term by a factor of e (i.e. 2.718). Such sensitivity in the rate at which thermal energy is converted into dissociation energy can be expected to significantly influence the flow field.

These influences can be explored through order of magnitude arguments, which are based on the assumption that temperatures can be reduced without limit. It must be admitted that the corresponding physical model becomes an increasingly extreme one as the temperatures are reduced, with a flow field of very large dimensions, in order to allow ξ to be large enough for dissociation to occur, and a very low density, in order to ensure that recombination does not occur. Such a model may not be strictly realizable, but may be expected to provide a good approximation to flight flow fields.

As a first step in using this low temperature approximation, it is worthwhile examining the relative order of magnitude of the two terms in the right hand side of Eqn. (6), in the context of the representative flow shown in Fig. 2. Considering the second term first, as the streamline which is shown in the figure passes around the body, it experiences a change in pressure which is of the order of the pressure itself. Thus, using Eqn. (5), the second term can be seen to be of the order of T/ξ_ℓ, where ξ_ℓ is the value of the binary reaction variable which is obtained for a distance along the streamline equal to a typical body length, ℓ. Then, if T_Q is the temperature at which the second term is of the same order as the first, Eqn. (3) yields

$$CT^{-n}\,(1 - \alpha)\,\exp(-T_Q^{-1}) \sim T_Q/\xi_\ell \quad ,$$

or, neglecting α compared with unity, and $(n + 1)\ell n\, T_Q$ compared with T_Q^{-1},

$$\exp(-T_Q^{-1}) \sim (\xi_\ell\, C)^{-1} \quad . \qquad (7)$$

Since ξ_ℓ and C are not sensitive to temperature, Eqn. (7) expresses the fact that the two terms on the right hand side of Eqn. (6) are of the same order only when $T \approx T_Q$. When $T < T_Q$, the second term in Eqn. (6) dominates, and the gas behaves as a perfect gas. When $T > T_Q$, the first term dominates, and Eqn. (6) then describes a relaxing dissociating gas which, because the pressure gradient is unimportant, is effectively decoupled from the flow field. The latter of these two cases will be discussed first, in the form of a constant pressure flow.

3. CONSTANT PRESSURE FLOW

If the pressure gradient term in Eqn. (6) is neglected, and it is combined with Eqn. (3), it becomes

$$dT/d\xi = -CT^{-n}\,(1+T)(1-\alpha)(4+\alpha)^{-1}\,\exp(-T^{-1}). \qquad (8)$$

For T sufficiently small, and regarding α as negligible compared with unity, this can be integrated to yield

$$\exp(T^{-1}) - \exp(T_0^{-1}) = 4C(\xi - \xi_0) \quad , \qquad (9)$$

where subscript "0" indicates a reference condition on the streamline. For Fig. 2, Eqn. (8) applies upstream of the point where $T \approx T_Q$, and therefore the reference condition, conveniently, may be taken at the shock. The first term on the left hand side of Eqn. (9) then becomes much larger than the second at a distance from the shock which is sufficient for the temperature to fall by only a small amount, and Eqn. (9) can be written

$$\exp(T^{-1}) \approx 4C\,\xi \qquad (10)$$

There are two important features of Eqn. (10). The first is that the small values of T ensure that large increases in ξ are necessary to effect small decreases in T. Repeating the example used for Eqn. (3), if $T \approx 0.05$, then ξ must increase by a factor e in order to decrease T by 5%. Thus, over any decade of ξ there is only a small variation of T, and it is a good approximation to regard T as constant. This implies that the temperature is approximately constant over most of any constant pressure flowfield, as illustrated in Fig. 3(a).

Fig. 3(a) also illustrates a corollary of this constant temperature approximation - namely, that nearly all of the temperature decay from T_o occurs close to the shock and, for purposes of approximate analysis, may be incorporated into the shock.

The second feature of Eqn. (10) is that T is independent of conditions at the shock and is, in fact, dependent only on ξ, which is approximately independent of the streamline enthalpy. Thus unlike a perfect gas flow, in which the temperature is coupled directly with the streamline enthalpy, the temperature in a dissociating gas flow is decoupled from the thermodynamics.

The reason for this can be seen by reference to Fig. 3(a). When the streamline enthalpy is raised from one level to a higher one, the temperature at the shock is increased but, by virtue of the exponential term in Eqn. (8), the reaction rate is greatly enhanced. This ensures that the temperature falls very rapidly along the streamline and therefore that it quickly returns to values associated with the lower enthalpy within a short distance from the shock. Essentially, the reaction processes initially take place at a much higher rate than the flow processes, but the strong exponential term ensures that the reaction rate is driven down until it matches the flow processes.

The constant temperature approximation and thermodynamic decoupling each offers a means of making simple approximate calculations of non-equilibrium real gas flows. Some examples of such calculations follow.

4. CONSTANT TEMPERATURE APPROXIMATION

(a) Shock Stand-off on a Sphere

The pressure in the shock layer on a sphere varies as $\cos^2\beta$, and therefore the flow sufficiently close to the stagnation point may be regarded as a constant pressure one. The constant temperature approximation then implies that the density may be taken to be approximately constant within the shock layer, and the shock stand-off distance calculated by using the relation for constant density flow presented in ref.3, i.e.

$$\Delta/a = 0.78\,\rho_\infty/\rho_s. \qquad (11)$$

Determination of T requires selection of an appropriate value of ξ. Since the sonic point at the shock occurs near $\beta = 30^0$, the arc length corresponding to $\beta = 15^0$ is a suitable value of s, whilst the velocity can be taken as the value immediately downstream of the normal shock.

Calculations using this method are compared in Fig. 4 with results of computational simulations for dissociating nitrogen. The computations were performed by Hornung (1979), and are seen to produce stand-off values which generally are within 10% of the computed values.

(b) Shock Detachment on a Wedge

As the vertex angle of a two dimensional wedge is increased, a point is reached at which the shock detaches and, with further increase in wedge angle, moves upstream of the vertex of the wedge. This effect is sensitive to the shock layer to free stream density ratio, and therefore is subject to real gas effects. Since the Newtonian pressure is constant on each of the faces of the wedge, it approximates to a constant pressure flow, and the constant temperature approximation will again apply.

In Fig. 5, calculations of shock detachment for nitrogen are compared with experimental results obtained by Hornung and Smith (1979). The shock detachment was obtained by using experimental results for argon, obtained at a Mach number of 16, which also are shown on Fig. 5. These results were used to predict nitrogen shock detachment by employing the three dimensional blunt body transformations of Stalker (1986) i.e. by putting

$$\left(\sqrt{\rho_s/\rho_\infty - 1}\ \cot\delta\right)_A$$

$$\left(\sqrt{\rho_s/\rho_\infty - 1}\ \cot\delta\right)_N,$$

and

$$\left(\sqrt{\rho_s/\rho_\infty - 1}\ \Delta/w\right)_A$$

$$= \left(\sqrt{\rho_s/\rho_\infty - 1}\ \Delta/w\right)_N$$

where A and N signify the argon and nitrogen flows respectively.

As seen on the figure, the resulting prediction of shock detachment is close to the experimental values, except near detachment. There the small scale of the detachment region is expected to change the effective value of ξ. Predictions of detachment for a perfect gas, with ratio of specific heats of 1.4, and for an equilibrium real gas also are shown. The non-equilibrium detachment is well removed from either of these two extremes.

5. THERMODYNAMIC DECOUPLING

Equation (10) has been used to argue that, because ξ is only weakly dependent on the streamline enthalpy, T is independent of the flow thermodynamics. This implies that the temperature is approximately independent of the shock angle and flight speed.

As a test of this conclusion, some experimental measurements of shock stand-off at the midplane of delta wings in air are presented in Fig. 6. Whilst the reactions involving nitric oxide make the chemistry of air somewhat more complicated that that of an ideal dissociating gas, the net dissociation rates at the temperature of interest in sub-orbital flight yield effects which are not dissimilar to the dissociation of pure oxygen, and so thermodynamic decoupling of the temperature also is expected for air.

Fig. 6(a) shows the effect of varying shock angle by varying the angle of incidence of the wing at a fixed stagnation enthalpy (Stalker, 1982). It is seen that when the measured shock stand-off at $\beta = 50^0$ is used as a reference condition, the constant temperature assumption can be used to make a satisfactory prediction of shock stand-off variation for a perfect gas, where the shock layer density, rather than the temperature,

is constant, and this is seen to produce a distinctly different result.

Fig. 6(b) shows the effect of varying the flight speed, by varying the flow stagnation enthalpy. The constant temperature curve employed the same reference condition as in Fig. 6(a), and is consistent with the experiments at 20 MJ.kg^{-1} and 30 MJ.kg^{-1}. At higher enthalpies, corresponding to super-orbital flight speeds, the gas in the shock layer approaches complete dissociation, and temperatures may be expected to exceed the reference value. This is evident in the experimental shock stand-off at 38 MJ.kg^{-1} where constant temperature calculations indicate that 90% of the air molecules are dissociated. Constant temperature calculations also indicate complete dissociation at 45 MJ.kg^{-1}, and it can be seen that a calculation based on the assumption of complete dissociation tended towards the experiments at the highest stagnation enthalpy tested.

6. FLOW WITH PRESSURE GRADIENT

Returning to Fig. 2., and recalling the discussion of Section 2, the effect of a falling pressure along a streamline was to cause dissociation to cease at a temperature, T_Q, which is given by Eqn. (7). Further cooling ensures that the dissociation reaction is even further checked. That is, the reaction is "quenched". Downsteam of the point where this occurs, the gas behaves as a perfect gas.

This process is represented graphically in Fig. 3(b), where it is seen that the effect of dissociation (i.e. "$d\alpha/dx$ contribution") dominates the cooling rate close to the shock but, when the pressure gradient becomes significant, the effect of dissociation is eliminated within a very short distance. That is, the quenching is "sudden".

Now, for the part of the streamline which is upstream of the quenched region, the gas behaves as if it were in a constant pressure flow and, taking ξ_ℓ once gain as the value of ξ corresponding to a typical body length, ℓ, it follows that the temperature, T_ℓ , over most of the flow for the constant pressure case is given by Eqn. (10), i.e.

$$\exp(T_\ell^{-1}) \approx 4C\ \xi_\ell$$

when this is compared with Eqn. (7), it is seen that

$$\exp(T_\ell^{-1}) \sim 4\ \exp(T_Q^{-1}) \quad ,$$

which can only be true if

$$T_Q - T_\ell \sim T_\ell\ T_Q \quad ,$$

$$\text{i.e. } T_Q \approx T_\ell \qquad (12)$$

Thus, the reaction quench temperature is approximately the same as that obtained by allowing the gas to relax in a constant pressure flow over a body of the same size, at the same density and velocity.

A further result follows from the comparison between flows with and without pressure gradient. In the case of the zero pressure gradient flow, it has already been remarked that almost all of the temperature change along the streamline takes place close to the shock. Since the flow with pressure gradient behaves like a constant pressure flow upstream of the quenched region, nearly all of the temperature change must occur near the shock in that case also, and a close approximation to the quench temperature must be achieved near the shock.

Hornung (1976) has performed a more rigorous analysis of the quenching effect, and finds that

$$T_Q = \sigma\{1 + \sigma \ln \sigma + \sigma \ln (1 + 4T_Q) + O(\sigma^2)\} \qquad (13)$$

where

$$\sigma^{-1} = \ln \{(1 - \alpha)T^{-n}\ \rho\ CR\ \tan\phi\ (3\ u_\infty\ \cos\phi)^{-1}\}$$

In both Eqn. (7) and Eqn. (13), it is clear that the dominant term is the large constant C and, for a strong bow shock without order of magnitude variations in the shock radius of curvature, T_Q is approximately constant. Thus, the constant density ratio strong shock generated in a perfect gas is replaced by a constant temperature ratio one in a non-equilibrium gas.

Hornung (1976) has presented experimental measurements which support the concept of a constant temperature shock. However, a second aspect of interest is that the quenched gas is expected to expand as a perfect gas as it passes along streamlines, and this will affect conditions downstream. This is illustrated in Fig. 7, where the results of numerical calculations supplied by Macrossan are presented. These were made by the equilibrium flux method, which has been outlined and validated by comparison with experimental results by Macrossan and Stalker (1987). The calculations showed that the dissociation fraction remained approximately constant along any streamline downstream of the shock wave. Contours of pressure are shown on Fig. 7(a), as well as a pressure profile across the shock layer at the trailing edge of the wedge surface, and they indicate that pressure ratios are approaching the asymptotic value of 50 for that wedge.

Shock layer profiles of flow parameters at the trailing edge are shown in Fig. 7(b). In order to indicate the extent of the departure from equilibrium, pseudo-equilibrium values of α and T have been obtained by allowing a gas sample to relax to equilibrium without altering its internal energy or density. When these are compared with the calculated profiles, it can be seen that the gas is considerably removed from equilibrium particularly on the streamlines close to the surface, which have passed through the strongest part of the bow shock. The downstream effect of quenching on fluid dynamic variables is shown in the profiles of density where it is seen that the quenched density profile, which is obtained by using Eqn. (13) to yield the shock temperature and then expanding as a perfect gas along streamlines downstream of the shock, agrees satisfactorily with the numerical results. For comparison, pseudo-equilibrium and perfect gas profiles of density for the same shock shape and trailing edge pressure profile are also shown, and are seen to differ substantially from the numerical results. For interest, velocity profiles also are displayed, and they show the increase in vorticity towards the surface which is associated with the dissociation.

7. CONCLUSION

A simplified gas model has been used to discuss aerodynamic effects associated with the flight of some simple vehicle configurations at velocities which are high enough to produce strong dissociation effects. The gas model involves a Lighthill-Freeman ideal dissociating gas, with the recombination effect removed. The small magnitude of the reduced temperature, T, has been exploited to emphasize the dominant role of the exponential term in the expression for the forward reaction rate. This has made it possible to develop

approximate concepts which identify the dominant non-equilibrium effects for these simple configurations.

One important feature has emerged which applies to nearly constant pressure flows, such as blunt bodies or nearly flat heat shields at incidence. Whereas such configurations would exhibit an essentially constant density shock layer in a perfect gas, with the density as a fixed multiple of the upstream density, the shock layer in dissociating gas is a constant temperature one. The temperature of the shock layer is determined by the value of the binary reaction variable, ξ. This approximation is seen to be effective in predicting the shock stand-off on a sphere.

It follows from this constant temperature approximation that all blunt body flows are essentially constant density ones, whether they be perfect gas, non-equilibrium, or equilibrium flows. This is illustrated by using perfect gas results with argon to predict the non-equilibrium shock detachment distance on a wedge in dissociating nitrogen.

The dependence of the shock layer temperature on the binary reaction variable, ξ, implies that it is decoupled from the streamline enthalpy. This, in turn, means that the temperature in the shock layer is independent of flight speed and incidence. This concept is seen to allow satisfactory prediction of the variation of shock stand-off with incidence on a delta wing in air. It is also consistent with the observed variation of shock stand-off with stagnation enthalpy, and thus flight speed, provided that the air in the shock layer does not approach complete dissociation.

The constant temperature feature also applies to the flow immediately downstream of a curved bow shock, producing an effective post-shock temperature which is independent of the local angle which the shock makes with the mainstream. The constant density ratio shock wave of a perfect gas flow thereby is replaced by a constant temperature ratio one. Downstream of the shock wave, the reactions in the gas are quenched, and perfect gas behaviour results. This model of the flow is confirmed by numerical simulation of the flow over a blunt wedge.

These simple flows demonstrate that dissociation of the flight medium can substantially modify the flow field about a vehicle. When these modifications are viewed in the light of the role of the exponential term in the dissociation rate equation, they are seen to lead to an interesting new set of principles to be applied to dissociating flows. There are many problems yet to be resolved which involved dissociating flow over flight vehicles - for example, leeward body flows, or detailed flows within the shock layer. It is not unreasonable to hope that these principles may be of service in approaching such problems.

ACKNOWLEDGEMENT

A substantial part of this work was supported by the Australian Research Grants Scheme.

NOTATION

a	sphere radius
C	reaction constant (Eqn. 1))
D	dissociation energy per unit mass
h	enthalpy per unit mass
n	pre-exponential temperature index
p	pressure
q	velocity along streamline
s	distance from shock along streamlines
T	reduced temperature - θ_d^{-1} x actual temperature
T_Q	reduced quench temperature
u_∞	mainstream velocity
w	wedge face length
α	degree of dissociation
β	angle between surface normal and mainstream
δ	wedge semi-vertex angle
Δ	shock stand-off distance
θ_d	characteristic temperature for dissociation
ξ	binary scaling variable (Eqn. (2))
ρ	density
ρ_d	characteristic dissociation density
ρ_s	density at distance s

Subscripts

∞	upstream
o	at the shock

References

FREEMAN, N.C., Non-equilibrium flow of an ideal dissociating gas. Journ. Fluid Mech. V4 pp 407 -425 (1958).

HORNUNG, H.G. Non-equilibrium dissociating nitrogen flow over spheres and circular cylinders. Journ. Fluid Mech Mech. V53 pp 149-176 (1972).

HORNUNG, H.G., Non-equilibrium ideal gas dissociation after a curved shock wave Journ. Fluid Mech. V74 pp 143-159 (1976).

HORNUNG, H.G. and Smith, G.H., The influence of relaxation on shock detachment Journ. Fluid Mech. V93 pp 225-239 (1979).

MACROSSAN, M.N. and Stalker, R.J., Afterbody flow of a dissociating gas downstream of a blunt nose AIAA paper 87-0407. Presented at Aerospace Sciences Meeting, Reno, Navada, Jan 1987.

STALKER, R.J. Non-equilibrium flow over delta wings with detached shock waves AIAA J. V20 pp 1633-1639 (Dec 1982).

STALKER R.J. A similarity transformation for blunt body flows AIAA Paper No. 86-0125. Presented at 24th Aerospace Sciences Meeting, Reno, Nevada, Jan 6-9, 1986.

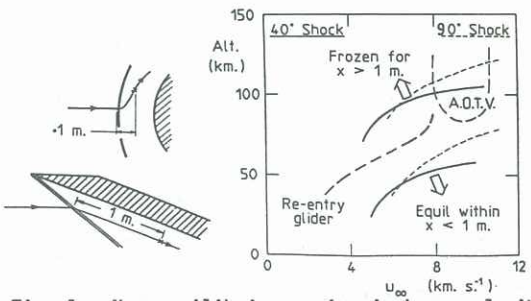

Fig. 1 Non-equilibrium regime in hypervelocity flight.

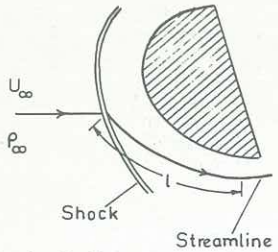

Fig. 2 Typical dissociating flow field.

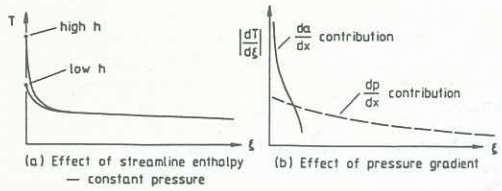

Fig. 3 Decay of reaction rate

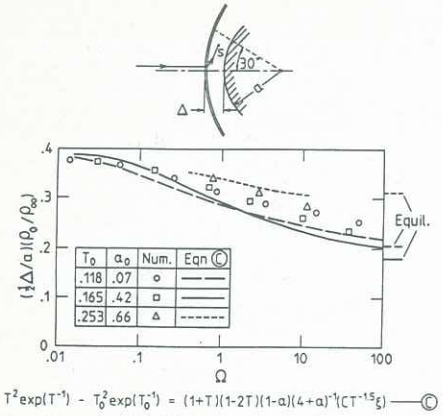

Fig. 4 Stand-off distance on sphere

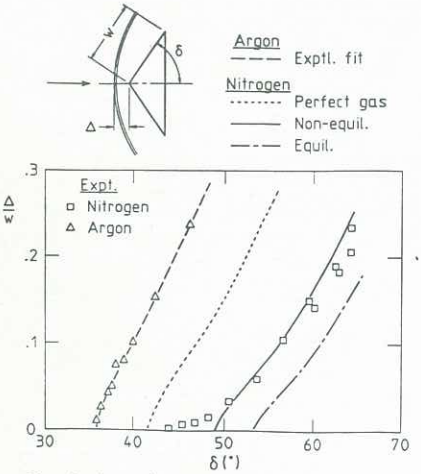

Fig. 5 Shock detachment on a wedge (Nitrogen test gas, u_∞ = 5.5 km s^{-1} ρ_∞ = 0.0026 kg.m^{-3}, α_∞ = 0.1, Mach no. = 7.5)

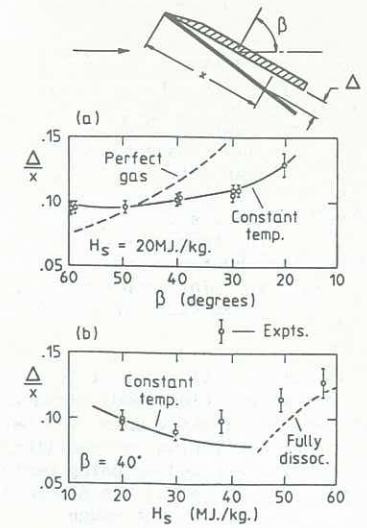

Fig. 6 Thermodynamic decoupling - shock stand-off on flat delta wing (H_S = stagnation enthalpy, L.E. sweep = 75°.

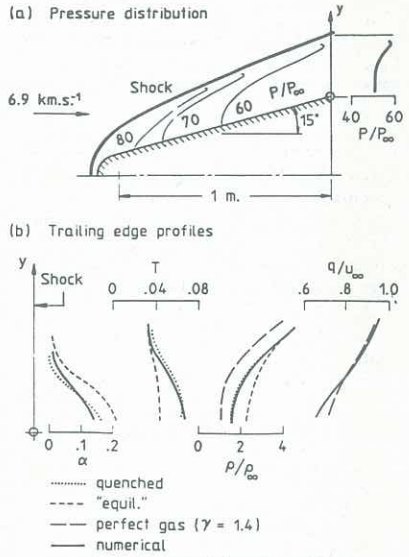

Fig. 7 Reaction quenching in nitrogen - effect on afterbody flow ($\rho_\infty = 10^{-4}$ kg.m^{-3}, α_∞ = 252K, r_n = 0.1m.)